Nilsén, Frans; Aaltio, Ilkka; Ge, Yanling; Lindroos, Tomi; Hannula, Simo-Pekka

Characterization of Gas Atomized Ni-Mn-Ga powders

Published in:
Materials Today: Proceedings

DOI:
10.1016/j.matpr.2015.07.422

Published: 01/01/2015

Document Version
Publisher's PDF, also known as Version of record

Available online at www.sciencedirect.com

ScienceDirect

materialstoday: PROCEEDINGS

Materials Today: Proceedings 2S (2015) S879 – S882

International Conference on Martensitic Transformations, ICOMAT-2014

Characterization of gas atomized Ni-Mn-Ga powders

F. Nilsén[a,]*, I. Aaltio[a], Y. Ge[a], T. Lindroos[b], S.P. Hannula[a]

[a]*Aalto University, Department of Materials Science and Engineering, Vuorimiehentie 2 A, 02150 Espoo, Finland*
[b]*VTT Technical Research Centre of Finland, Tekniikankatu 1, 33100 Tampere, Finland*

Abstract

Gas atomization is a well-known process for obtaining high quality metallic powders. It produces spherical high-density particles with a controllable particle size distribution. We used gas atomization to obtain two different Ni-Mn-Ga powders and investigated their microstructure, transformation temperatures and magnetic properties as well as the effects of heat treatment on those. The phase and magnetic transformation temperatures of the powders were considerably lower as compared to similar conventionally prepared alloys. Nevertheless, heat treatment of the atomized powder was found to recover the magnetic properties of the materials, probably by releasing the residual strains generated by the rapid solidification during the gas atomization process. Sintering of powders seemed to start at a significantly lower temperature when compared to the powder prepared by ball milling of bulk Ni-Mn-Ga-alloys.

Selection and Peer-review under responsibility of the chairs of the International Conference on Martensitic Transformations 2014.

Keywords: Ni-Mn-Ga; gas atomization; magnetic properties; microsturcture

1. Introduction

Ni-Mn-Ga alloys have attracted much attention as a magnetic shape memory material when it was found that martensitic single crystal Ni-Mn-Ga alloys are capable of achieving reversible magnetic-field-induced strains (MFIS) of up to 10% [1-4]. The MFIS is due to martensitic twin variant redistribution, where the martensitic variant oriented most favorably to external magnetic field grows at the expense of other twin variants [5, 6]. One of the

* Corresponding author. Tel.: +35850-433-4173;
E-mail address: frans.nilsen@aalto.fi

Selection and Peer-review under responsibility of the chairs of the International Conference on Martensitic Transformations 2014.
doi:10.1016/j.matpr.2015.07.422

problems with Ni-Mn-Ga alloys is that the highest MFIS have been achieved only with costly and hard to manufacture single crystals, due to the constraints imposed by the grain boundaries to twin boundary motion in polycrystals [7-9]. An alternative approach to reach high MFIS is to create a porous structure, where grain boundary constraints are smaller than e.g. in dense polycrystals [9, 10]. Porous structures may be produced e.g., by controlled casting [11] or sintering of powders [12]. MSMA powders with irregular particle shape have been previously prepared successfully by ball milling [13, 14]. Nevertheless, gas atomization can be used to produce regularly shaped, smooth and dense particles, with a more accurate control of particle size and lower sintering temperature [15, 16]. In this paper we report the properties of gas atomized Ni-Mn-Ga alloy powders and the effect of subsequent heat treatment on them. In particular, we study the magnetic properties, transformation temperatures, sintering temperatures, and the crystal and microstructure of the powders.

2. Experimental & Results

VTT Technical Research Centre of Finland produced two batches of gas atomized powder (marked as ATO1 and ATO2), with Hermica gas atomization equipment using pre-alloyed starting materials. The ATO1 alloy was atomized at 1353 K using a melt chamber pressure of 0.3 bars and atomization pressure of 40 bars. For ATO2 the corresponding parameters were 1581 K, 0.25 bars and 50 bars. The diameter of the atomization nozzle was 1.5 mm and the atomization gas was argon. ATO1 pre-alloy composition was $Ni_{49.0}Mn_{26.5}Ga_{25.5}$ and the end composition of the ATO1 powder was $Ni_{49.7}Mn_{27.6}Ga_{22.8}$. In the case of ATO2 the pre-alloy composition was $Ni_{49.6}Mn_{29.2}Ga_{21.3}$ while the end composition of ATO2 powder was $Ni_{49.3}Mn_{28.8}Ga_{21.6}$. With ATO2 pre-casting into a copper mould introduced 0.3 at% of copper to the material. The powders were sieved in the case of ATO1 below 150 µm and in the case of ATO2 below 75 µm and it led to average particle size of 24.4 µm. Finer sieving was used with ATO2 powder due to impurity element particles found in the EDS study which lead to average particle size of 15.2 µm, in the case of ATO1 no impurities were found. Higher atomization pressure in the ATO2 process led to a larger amount of smaller particles. This was expected since the particle size in gas atomization depends mainly on gas to metal ratio during the process, which in turn is affected mostly by the atomization pressure and to a lesser degree by melt chamber pressure and atomization temperature [15]. Gas atomized powders were placed into evacuated quartz ampoules, which were then heat treated at different temperatures. One sample for 24 hours, two samples for 144 hours and one for 240 hours, while one sample from both batches was left without heat treatment (NHT). The heat treatment temperatures (Fig. 1) were chosen below the expected melting temperature of 1353 K to avoid possible sintering of the powder. The powders were not mixed during the heat treatments. During heat treatment three different structures were formed from powder; (i) powdery, (ii) partly sintered mesh-like and (iii) a fully sintered structure. ATO1 remained in a powdery form under 1023 K. Between the heat treatment temperatures of 1023 K and 1273 K the ATO1 powder changed to partly sintered and porous mesh-like structure until the powder sintering fully at 1273 K. With ATO2 even the initial heat treatment at a temperature of 873 K led to partial sintering. The powder densified with the rising temperature until the powder sintered fully at 1173 K and higher. This was unexpected since with milled particles sintering at such low temperatures has previously required pressure around 50 MPa and a pulsed current with electric pulse/pause ratio of 10:5 ms [14]. The martensitic and

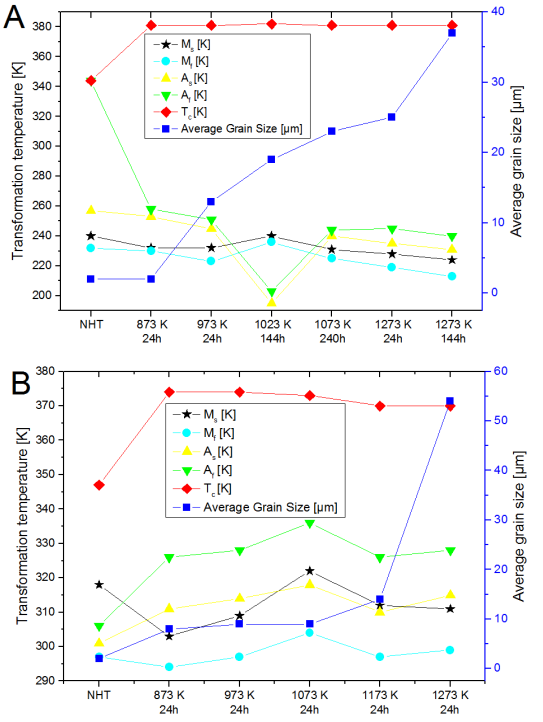

Fig. 1. Transformation temperatures obtained by DSC and magnetic susceptibility measurements and average grain size for (a) ATO1 and (b) ATO2

austenitic start and end temperatures (M_s, A_s, M_f and A_s) and Curie temperature (T_c) were determined with a laboratory made low-field AC magnetic susceptibility measurement system. Temperature change rate for the experiment was 5 K/min and the samples were cycled between temperatures of 153 K and 393 K five times. Transformation temperatures were confirmed using a Linkam-600 differential scanning calorimeter (DSC) system with a cooling rate of 2 K/min for ATO1 and 3 K/min for ATO2. Samples were first heated to 283 K and then cooled to 153 K in the case of ATO1 and to 253 K in the case of ATO2; a sapphire crucible was used for the powdery samples. Since the Curie temperature depends in addition to the materials chemical composition on the ordering of $L2_1$-phase, the significant difference in T_c change between the non-heat treated and the heat-treated material can be attributed to the structural ordering of the crystal structure and relief of internal stresses that happens during heat treatment [13]. In ATO1 powder the transformation temperatures (Fig.1) remained unchanged after heat treatment at 873 K, which relieved the residual internal strains formed at the atomization process. In ATO2 as the powder becomes partly sintered and a porous mesh-like structure appears at 1073 K, the M_s and the M_f rise abruptly. After the powder sinters fully at 1173 K both transformation temperatures, M_s and M_f, descend closer to the M_s and M_f temperatures of the NHT sample. Changes in the transformation temperatures of ATO2 could be due to the copper impurity [17].

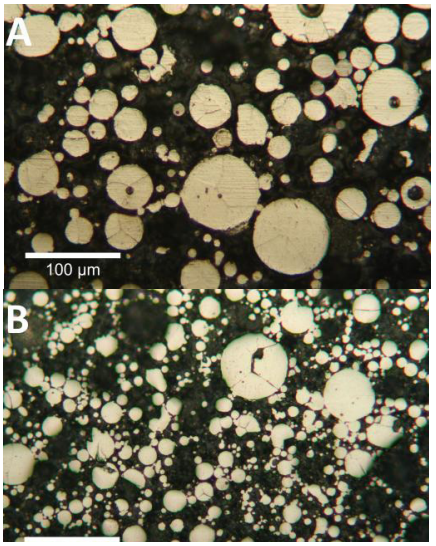

Fig. 2. Cross sections of powders after heat treatment at 1073 K. (a) ATO1 after 240 h and (b) ATO2 after 24 hours.

Microstructures were studied using optical microscope Leica DMRX and scanning electron microscope (SEM) Tescan Mira3. Samples were mounted in EpoFix epoxy, then ground and polished, first with diamond paste with particle sizes 6, 3 and 1 µm and then by etching with 10% Nital (Fig. 2). As can be seen in ATO1 grain growth occurs faster than that in ATO2 at the same heat treatment temperatures (Fig. 2). However, in ATO2 the grain size of the material after heat treatment at 1273 K for 24 hours is more than twice as large as that of ATO1 after the same treatment (Fig. 1). At the beginning of the densification process particles started forming larger agglomerates of smaller particles and when heat treatment was continued these agglomerates grew until powder was fully sintered. Heat treating ATO1 powder at 1073 K for 240 hours lead to almost the same grain size as heating it for 24 hours in 1273 K. Comparing the transformation temperatures (Fig. 1) and magnetization (Fig. 3a) of these two different samples it can be seen that there is only a small difference in transformation temperatures and no difference in materials magnetization. Thus no added benefit can be obtained by using longer heat treatment time or higher temperature. The EDS results from the powder heat treated at 1073 K show that ATO1 composition is $Ni_{50.2}Mn_{26.7}Ga_{23.1}$ after 240 hours of heat treatment while ATO2 composition after 24 hours is $Ni_{49.7}Mn_{28.4}Ga_{21.9}$. The EDS was measured using a $Ni_{50.0}Mn_{26.6}Ga_{23.4}$ sample with known composition as a standard. This small change in composition compared to the non-heat treated powders can be explained by the homogenization of the structure during heat treatment. The room temperature crystal structure of the powders was studied using PANanalytical X'Pert Pro XRD and analyzed using X'Pert Highscore Plus. Both ATO1 and ATO2 showed cubic structure with a weak $L2_1$ order before any heat treatments. The cubic lattice parameter for ATO1 is a = 5.83 Å and for ATO2 a = 5.84 Å. Due to

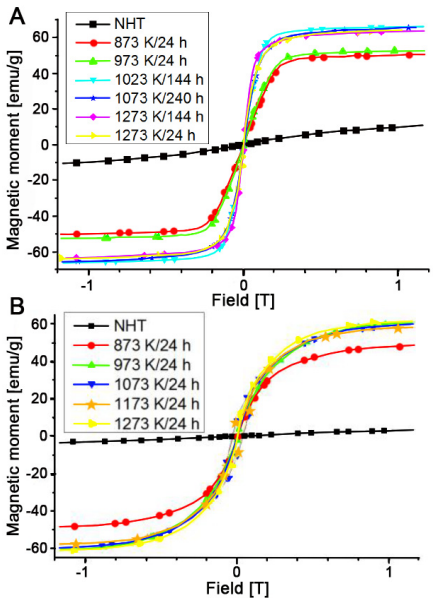

Fig. 3. VSM magnetic moment curves from different heat treatments for (a) ATO1; (b) ATO2

different composition, the martensitic transformation temperature of ATO1 is below room temperature and ATO2 is above room temperature (Fig. 1). Thus all the XRDs of ATO1 showed the cubic structure. After heat treatment, the ATO2 was found to be martensite at room temperature. The martensite of ATO2 is a five-layered modulated structure with lattice parameters: a = 4.22 Å, b = 5.60 Å, c = 21.00 Å and β = 90.2° for the modulated unit cell. Heat-treating powders removed internal stresses and led to higher structural ordering.

The magnetization of both powders was studied at room temperature using laboratory made vibrating sample magnetometer (VSM) where the magnetic field strength was cycled between -1.2 T and 1.2 T, the vibration amplitude was constant and frequency 20 Hz. A NIST nickel magnetic moment standard disk was used as a calibration sample and the specimen were weighted before the experiment. In both powders heat treatment was found to recover the ferromagnetic properties of the material (Fig. 3). The magnetic moment of both ATO1 and ATO2 increased with the heat treatment temperature; with ATO1 the maximum values were found with heat treatment temperatures over 1023 K (Fig. 3a) and with ATO2 at heat treatment temperatures over 873 K (Fig. 3b). A difference can also be seen in the saturation field values; ATO1 reaches saturation with field of 0.3 T while ATO2 reaches saturation point at approximately 0.8 T. In both ATO1 and ATO2 it can be seen that the magnetic moments of the as-atomized powder samples are smaller than with the heat-treated samples. This is due to reorganization of the $L2_1$ structure and the relief of internal stresses that happens during heat treatment [13]. The highest magnetic moment of ATO1 is approximately 65 emu/g, which is slightly higher than that reported earlier for directionally solidified cubic austenite phase (60 emu/g [5]) having roughly the same composition. The highest magnetic moment of ATO2 is approximately 61 emu/g being somewhat lower than that reported for 5M Ni-Mn-Ga (64 emu/g [5]).

3. Conclusions

Gas atomization produces highly spherical, small and fine-grained Ni-Mn-Ga powder. Additionally, gas atomization lowers the sintering temperature of the material in comparison to the ball milled powder. Heat treatment of the powder relieves residual internal stresses created by the atomization and recovers the magnetic properties of the material. Heat treatment of the powders brought the transformation temperatures closer to room temperature in both powders studied, the exception being the ATO2 powder heat treated at 1073 K.

Acknowledgements

We gratefully acknowledge Academy of Finland for the funding of this work (Project no. 259235).

References

[1] M. Chmielus, X.X. Zhang, C. Witherspoon, D.C. Dunand, P. Müllner, Nat. Mater. 8 (2009) 863–866
[2] O. Söderberg, A. Sozinov, Y. Ge, S.P. Hannula, Handbook of Magnetic Materials, Elsevier, Netherlands, 2006, p. 1–40.
[3] O. Söderberg, M. Friman, A. Sozinov, N. Lanska, Y. Ge, M. Hämäläinen, V.K. Lindroos, Z Metallkd 95 (2004) 724–731.
[4] O. Söderberg, I. Aaltio, Y. Ge, O. Heczko, S-P. Hannula, Mat. Sci. Eng. A-Struct. 481-482 (2008) 80–85.
[5] O. Heczko, N. Lanska, O. Söderberg, K. Ullakko, J. Magn. Magn. Mater. 242-245 (2002) 1446–1449.
[6] I. Aaltio, M. Lahelin, O. Söderberg, O. Heczko, B. Löfgren, Y. Ge, J. Seppälä, S.P. Hannula, Mat. Sci. Eng. A-Struct. 481-482 (2008) 314–317.
[7] D.L. Schlagel, Y.L. Wu, W. Zhang, T.A. Lograsso, J. Alloys Comp. 312 (200) 77–85.
[8] P. Müllner, X. Zhang, Y. Boonyuongmaneerat, C. Witherspoon, M. Chimielus, D.C. Dunand, Mater. Sci. Forum 635 (2010) 119–124.
[9] X.X. Zhang, M. Chimielus, C. Witherspoon, D.C. Dunand, P. Müllner, Nat. Mater. 8 (2009) 863–866.
[10] Y. Boonyuongmaneerat, M. Chimielus, D.C. Dunand, P. Müllner, Phys. Rev. Lett. 99 (2007) 247201.
[11] D. Jiang, S. Lixin, M. Jeong, M. Selke, F. Zhou, Adv. Sci. Lett. 6 (2012) 189–194.
[12] A. Bansiddhi, D.C. Dunand, Acta Biomater. 4 (2008) 1996–2007.
[13] B. Tian, F. Chen, Y. Liu, Y.F. Zheng, Intermetallics 16 (2008) 1279–1284.
[14] O. Söderberg, D. Brown, I. Aaltio, J. Oksanen, J. Syrén. H. Pulkkinen, S.P. Hannula, J. Alloys Compd. 509 (2011) 5981–5987.
[15] W.B. Eisen, B.L. Ferguson, R.M. German, R. Iacocca, P.W. Lee, D. Madan, K. Moyer, H. Sanderow, Y. Trudel (Eds.), ASM Handbook Volume 07: Powder Metal Technologies and Applications, ASM International, USA, 1998, p. 111–122.
[16] A. Simchi, A. Rota, P. Imgrund, Mat. Sci. Eng. A-Struct. 424 (2006) 282–289.
[17] M. Zelen, A. Sozinov, L. Straka, T. Björkman, R.M. Nieminen, Phys. Rev. B 89 (2014) 184103–184112.